NANO LETTERS

LETTER

pubs.acs.org/NanoLett

Nanopore Translocation Dynamics of a Single DNA-Bound Protein

Andre Spiering, Sebastian Getfert, Andy Sischka, Peter Reimann, and Dario Anselmetti*

Fakultät für Physik, Universität Bielefeld, Universitätsstrasse 25, 33615 Bielefeld, Germany

ABSTRACT: We study the translocation dynamics of a single protein molecule attached to a double-stranded DNA that is threaded through a solid-state nanopore by optical tweezers and an electric field (nanopore force spectroscopy). We find distinct asymmetric and retarded force signals that depend on the protein charge, the DNA elasticity and its counterionic screening in the buffer. A theoretical model where an isolated charge on an elastic, polyelectrolyte strand is experiencing an anharmonic nanopore potential was developed. Its results compare very well with the measured force curves and explain the experimental findings that the force depends linearly on the applied electric field and exhibits a small hysteresis during back and forth translocation cycles. Moreover, the translocation dynamics reflects the stochastic nature of the thermally activated hopping between two adjacent states in the nanopore that can be adequately described by Kramers rate theory.

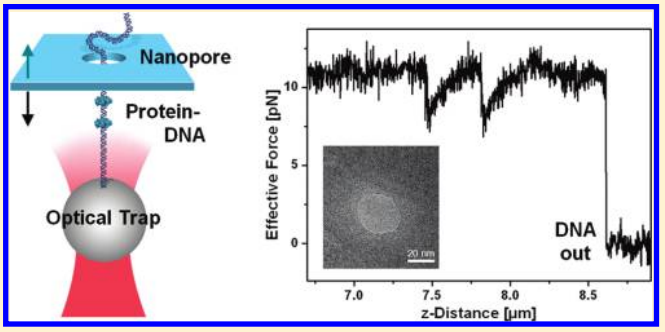

KEYWORDS: Single molecule, nanopore, optical tweezers, translocation dynamics, hysteresis, thermal fluctuations

The investigation and quantification of molecular translocation phenomena through nanopores (NPs) has gained widespread attention during the past decade.[1] Numerous applications were either developed or envisioned to monitor the translocation of individual molecules like nucleic acids or proteins through artificial solid state NPs for sieving,[2] biosensing,[3] and even DNA-sequencing[4−6] purposes. Therefore, Coulter counter based setups[7] were developed, where changes in electrical conductance of a NP are detected at remarkable sensitivity and time-resolution that could be statistically analyzed and attributed to molecular passages. Since in these confined fluidic environments with reduced dimensions concepts of micro- and nanofluidics apply, phenomena like Brownian motion, electrophoresis, electroosmosis, and electrostatic screening have to be considered.[8] Whereas in the early experiments the stochastic one-by-one translocation of denumerable molecules through solid-state NPs was statistically analyzed,[9] very recent experiments focus on the manipulation and translocation of an individual molecule (like DNA) that can be reversibly threaded in and out a NP, for example, by optical tweezers (OT).[10,11]

In this Letter, we report on the controlled translocation of a single protein molecule attached to a single double-stranded DNA through a Si_3N_4 solid-state NP by means of OT and an electric field under buffer conditions (single molecule NP force spectroscopy). Its associated charge-dependent experimental force response and dynamics are theoretically modeled within a framework of thermally activated transitions in a time-dependent two-state NP potential, accounting for the local electric field, its ionic environment, the optical trap stiffness, and the elasticity of the DNA.

We used a 3D quantitative OT system that allowed manipulation and steering of polystyrene microbeads under buffer conditions in a microfluidic nanopore cell as well as measurement of the minute piconewton forces acting on the bead (Figure 1a).[11] Our single-beam OT system is equipped with confocal light guiding that incorporates an optical obstruction filter eliminating all axial light components. The latter is imperative to carefully measure the small force contributions of a single translocating molecule since it significantly reduces unwanted interference signals from the thin membrane in backscattered light detection mode. Individual Lambda bacteriophage DNA molecules (48 502 basepairs (bp), 16.4 μm contour length) were functionalized at one end with several biotins and individually attached to a streptavidin-coated polystyrene bead. The DNA-bead constructs were kept in buffer solution (20 mM KCl and 2 mM Tris/HCl at pH 8.0) at 22 °C and introduced into our NP fluidic cell. The solid state Si_3N_4-membrane (20 nm thickness) was milled with a He-ion microscope (Zeiss, Oberkochen, D) rendering nanopore openings with typically 20−60 nm in diameter. The membrane was integrated into the fluidic cell so that the two sides of the membrane were only electrically contacted via the NP. In order to probe the force response of an individual protein attached to DNA when being threaded through a NP, we introduced either EcoRI (31 kDa, monomer) or RecA (38 kDa) proteins.

A representative first example for EcoRI is depicted in Figure 2, exhibiting a characteristic asymmetric force fingerprint (dip) with a retarded force increase extending over more than 200 nm. Qualitatively, these findings can be readily understood from the force balance indicated in Figure 1a and the fact that the externally applied voltage drop mainly occurs close to the pore: The concomitant electrical field "through" the pore generates a constant "pulling" force on the negatively charged DNA, visible as constant "background" force of about 11pN in Figure 2. While

Received: May 9, 2011
Revised: June 10, 2011
Published: June 13, 2011

dx.doi.org/10.1021/nl201541y | *Nano Lett.* 2011, 11, 2978–2982

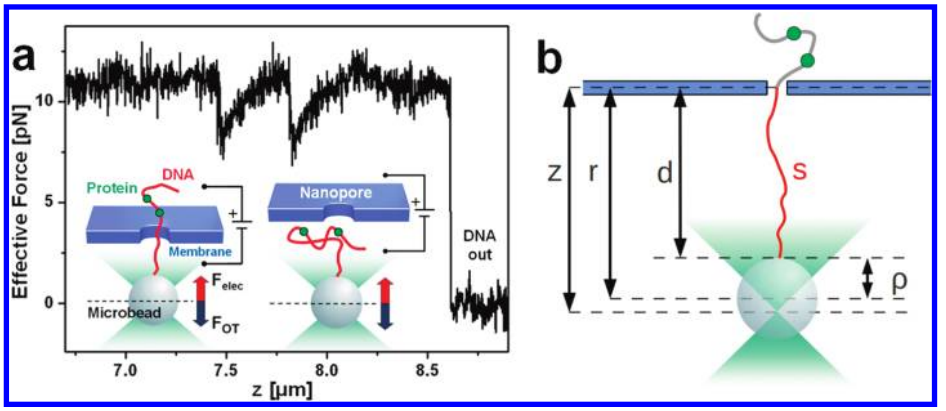

Figure 1. (a) Single molecule NP force spectroscopy: a microbead with an attached DNA molecule is optically trapped in the vicinity of a solid state NP. A membrane voltage drives the negatively charged DNA into the NP. The electrokinetic forces on the DNA are balanced by the force acting on the bead in the optical trap. The distance between trap and membrane can be continuously varied with nanometer precision. In the force−distance curve, two isolated DNA-bound proteins can be detected as distinct signals by unthreading the DNA strand out of the NP. (b) Illustration of the different length variables as used in the theoretical modeling.

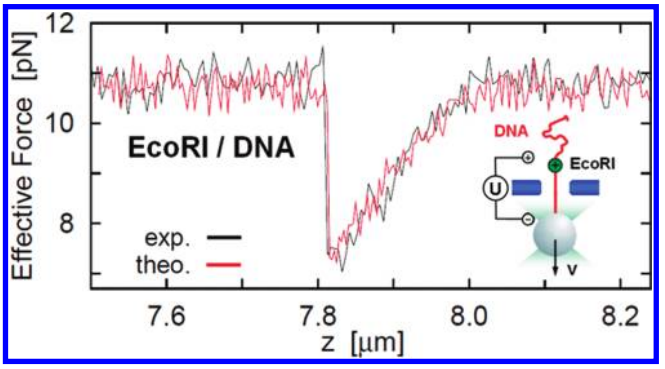

Figure 2. Force response of an individual EcoRI protein/DNA complex translocating through a solid state NP (45 nm pore diam.; $U = +50$ mV, constant threading velocity $\dot{z} = v$ of 100 nm/s. Black, experiment; red, theory).

the positively charged protein attached to the DNA is passing through the pore, this pulling force is temporarily reduced. More precisely, as the protein is approaching the pore, at some point the force equilibrium destabilizes and the protein moves very quickly through the pore toward a new force equilibrium at a reduced DNA-strain to be balanced by the OT ("downward jump" in Figure 2). As z further increases, the protein is steadily pulled away from the pore region and hence contributes less and less to the force equilibrium (increasing force in Figure 2).

Quantitatively, we model the setup from Figure 1a by means of two state variables: (1) the distance r between the bead center and the NP, and (2) the contour length s of the DNA segment between bead and NP (see graphical representation in Figure 1b). The optical trap at distance z from the NP exerts a force $F = \kappa(z - r)$ on the bead with an experimentally determined "elasticity" of $\kappa \simeq 0.05$pN/nm.[11] The corresponding trap potential is therefore $V_t(r) = (\kappa/2)(z - r)^2$. Likewise, the force on the charged DNA-strand derives from a potential $V_{DNA}(s) = \varepsilon s U$, where ε is the line charge density along the DNA and U the applied membrane voltage. Further, the DNA segment of length s between bead and NP gives rise to entropic forces, deriving from the wormlike-chain (WLC) potential[12] $V_{wlc}(r,s) = (kT/\lambda) \times [(s/4)\{(1 - (d/s))^{-1} - 1\} - (d/4) + (d^2/2s)]$, where $d = r - \rho$ with bead radius $\rho \simeq 1.64\ \mu$m is the relevant end-to-end distance of the DNA segment, $\lambda \simeq 50$ nm is its persistence length,[13] k is Boltzmann's constant, and $T \simeq 295$ K. Finally, the protein attached to the DNA is modeled as a point charge q and the associated electrostatic potential along the pore axis $\Phi(z)$ is numerically determined from Laplace's equation for a nonconducting plane, surrounded by a conducting liquid and exhibiting a pore, whose size and shape approximately emulate the experimentally known data. As already mentioned, one finds that $\Phi(z)$ is practically constant outside the immediate neighborhood of the pore. Assuming that in this region the DNA sojourns close to the pore axis, and s_p denotes the DNA contour length between bead and protein, it follows that $(s_p - s)$ is the relevant DNA contour length between protein and pore center, and $V_p(s) = q\Phi(s_p - s)$ the concomitant potential energy. Note that the latter also accounts for electroosmotic flow (EOF) due to a well-known "similitude" between electrophoresis and electroosmosis,[14] provided q is considered as a correspondingly renormalized (but still U-independent), "effective" charge. We further note that, since it is unknown where the protein attaches to the DNA, s_p is a fit parameter of our model.

Altogether, our state variables r and s are thus subject to the total potential

$$V(r,s) = V_t(r) + V_{DNA}(s) + V_{wlc}(r,s) + V_p(s) \qquad (1)$$

and their time evolution is governed by the Langevin dynamics

$$\eta_1 \dot{r} = -\frac{\partial V(r,s)}{\partial r} + \sqrt{2kT\eta_1}\xi_1(t)$$

$$\eta_2 \dot{s} = -\frac{\partial V(r,s)}{\partial s} + \sqrt{2kT\eta_2}\xi_2(t) \qquad (2)$$

As usual, in stochastic modeling[15,16] the friction coefficients $\eta_{1,2}$ and the δ-correlated Gaussian noises $\xi_{1,2}$ account for the dissipation and fluctuation effects of all the "fast" molecular degrees of freedom of the ambient fluid and of the DNA. Stokes friction of the bead (radius $\rho \simeq 1.64\ \mu$m) was calculated to $\eta_1 \simeq 3.1 \times 10^{-5}$ pNs/nm. For the corresponding (Stokes) friction of the DNA η_2, we estimated $\eta_2 \simeq 10^{-6}$pNs/nm, as adopted from ref 17.

Introducing our above explicit expressions for the various potentials on the right-hand side of eq 1, one finds that the total

dx.doi.org/10.1021/nl201541y |Nano Lett. 2011, 11, 2978–2982

NP potential $V(r,s)$ exhibits two minima (potential wells), corresponding to two metastable "states" in Figure 1 with the charged protein on either side of the membrane. This bistability is restricted to trap positions z within some finite interval, otherwise $V(r,s)$ from (1) exhibits a single well. As the trap z moves forward (downward in Figure 1), the dynamics (2) starts off with small thermal fluctuations of r and s about the accompanying single well of $V(r,s)$ ("state 1"). At some (bifurcation) point, a small secondary minimum of $V(r,s)$ is born ("state 2"), which subsequently deepens, while the original minimum is fading away. As a result, the dynamics (2) exhibits noise induced transitions from state 1 into state 2, accompanied by a "jump" of the force $F = \kappa(z - r)$, see Figure 2. In other words, we recover our previous qualitative picture of what is going on, but now also including all the quantitative details.

The actual values of ε and q depend in a very complex way on the real molecular charges and on their ionic environment via screening effects and EOF,[14,17,18] which in turn also depend on the pore geometry and material. In the absence of a quantitative theory, we estimated ε and q from the experimental data, yielding $\varepsilon \simeq -1.23e$/nm for the naked DNA (equivalent to $-0.41e$/bp) and $q \simeq +59.5e$ for a single protein EcoRI (Figure 2). Whereas the measured charge per DNA bp (bp-distance = 0.334 nm, nominal (bare) charge per bp = $-2e$) can be associated with an effective screening of $(1 - 0.41/2) = 0.79$, which nicely corresponds with earlier static experiments,[19] the measured effective protein charge is remarkably large and typically varies between $15 - 60e$ for DNA-bound EcoRI and different nanopores. The latter reflects different DNA−protein complex configurations as well as considerable EOF effects contributing via frictional forces along the DNA strand to the measured force equilibrium and hence affect the nominal effective charge q.[14,17,18] It is worth noting, that EcoRI is known to bind to DNA in specific and nonspecific ways[20] leading to several complex configurations where differently (charged) surface areas are exposed. In addition, the membrane charge density (mainly due to OH^- on Si_3N_4/SiO_2) inside the NPs varies between different NPs, leading to different EOF contributions. This variation in effective charge can directly be estimated from the measured peak area, corresponding to $\sim qU$.

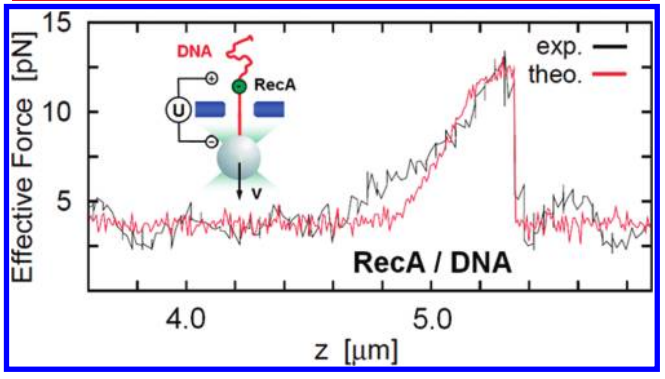

Figure 3. Force response of an individual RecA protein/DNA complex translocating through a solid state NP (45 nm pore diam.; $U = +20$ mV, threading velocity $v = 100$ nm/s. Black, experiment; red, theory).

As a second example, Figure 3 shows a typical force response curve for the protein RecA. Whereas EcoRI gives rise to a force "dip" (Figure 2), the signature of RecA is a force "peak" (Figure 3), which is moreover much broader. The reason is that the two proteins are oppositely charged and that unlike EcoRI, which can be assumed to bind to DNA as an isolated protein (see also Figure 1), RecA is known to bind cooperatively to DNA, forming negatively charged oligo- or multimeric assemblies.[10,21] In the theory, this fact is accounted for by replacing the point charge q with a charge density ε_p along a small DNA segment of length Δs_p. Our best fit in Figure 3 was obtained for $\varepsilon_p \simeq -2.8e$/nm and $\Delta s_p \simeq 250$ nm, resulting in a total effective protein charge of $-700e$. Assuming typically 50 RecA proteins in series, this would hint to an average effective charge of $\simeq -14e$ per protein, roughly corresponding to the determined effective (absolute) charge of the EcoRI protein.

Returning to EcoRI, Figure 4 shows the measured voltage dependency of the force signals, again in very good agreement with the theory. Clearly, an increase in membrane voltage U has three main effects: (i) The effective force acting on the naked DNA strand increases almost linearly with U. The tiny deviations from a strictly linear U-dependence are at the edge of the experimental uncertainties in Figure 4 and are correctly reproduced by the theory. (ii) The position of the force jump moves toward larger z-distances. According to our theory, the latter is not due to a real protein migration along the DNA strand, but rather due to an elastic DNA elongation and a displacement of the bead inside the optical trap as reaction to the larger electrical forces. (iii) As indicated above, the measured peak areas increase with the voltage according to qU.

In contrast to Figure 2, an entire back-and-forth translocation cycle in experiment and theory is presented in Figure 5, featuring a small but still clearly visible hysteresis of the force jump. Our theoretical explanation of the observed hysteresis is that the noise activated transitions between the two "states" of $V(r,s)$ according

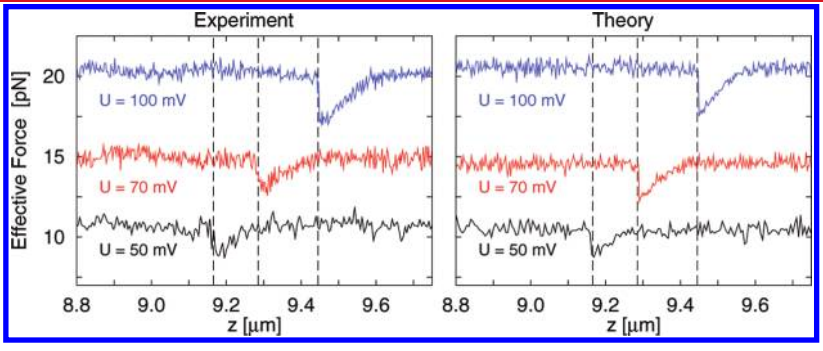

Figure 4. Voltage dependency of the force response signals (EcoRI/DNA, 30 nm pore diam., $v = 100$ nm/s. Left, experiment; right, theory). For details see text.

dx.doi.org/10.1021/nl201541y |*Nano Lett.* 2011, 11, 2978–2982

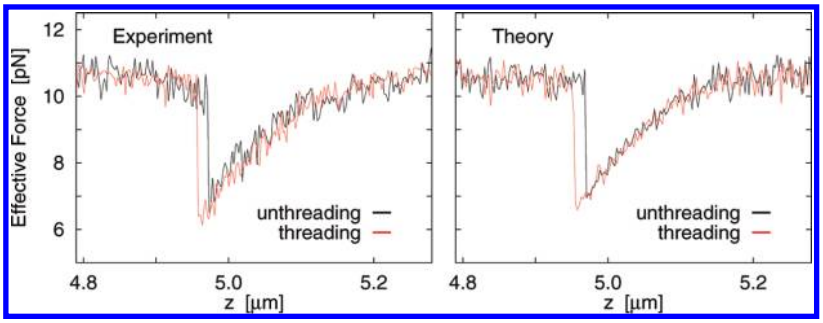

Figure 5. Force response signals of a threading and unthreading translocation cycle, exhibiting a small hysteresis in experiment (left) and theory (right). (EcoRI/DNA, 45 nm pore diam, U = +50 mV, v = ±100 nm/s). For details see text.

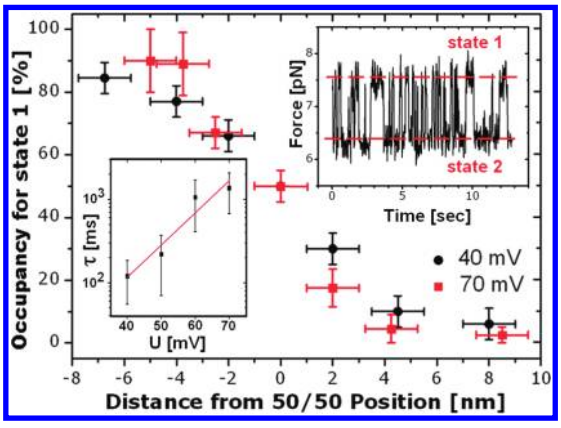

Figure 6. Upper inset: Time-dependent transitions between NP states 1 and 2 at a fixed trap position with 50/50 occupancy of both states (EcoRI/DNA, 50 nm pore diam, U = +40 mV). Lower inset: Voltage dependent mean residence time τ at 50/50 occupancy. Main plot: Distance dependence of state 1 occupancy for U = +40 mV (black) and U = +70 mV (red).

to eqs 1 and 2 are slower than the temporal changes of the potential $V(r,s)$ itself. Therefore, the actual transitions from "state 1" into "state 2" are "retarded" when z moves forward (unthreading), and exhibit an opposite "delay" upon threading. The corresponding intuitive picture is as follows: In Figure 1a, the negatively charged DNA-strand is pulled upward by the electrical field. As the microbead moves downward, the positively charged protein approaches the pore. As a consequence, the net electrical force on the DNA−protein complex diminishes until it is unable to counterbalance the pulling force exerted by the bead. At this moment, the protein slips through the pore and proceeds until a new stable force balance is reached, observable as downward jump inside the unthreading force signal of Figure 5. When the bead reaches the very same position on its way upward, the force balance is still stable. Only when the bead moves further upward, an analogous instability occurs, observable as upward jump inside the threading force signal.

In a next experiment, we experimentally fine-tuned the trap position z to a 50/50 occupancy of both states (upper inset of Figure 6) and determined the corresponding mean residence time τ within one state. The results for several different membrane voltages U are presented in the lower inset of Figure 6. According to Kramers rate theory[15] $\tau = \tau_0 \exp(\Delta E^{\ddagger}/kT)$, where the activation energy $\Delta E^{\ddagger}$ is approximately proportional to U and the prefactor τ_0 independent of U for our specific model potential $V(r,s)$ from (2). Figure 6 confirms this theoretical prediction yielding an activation energy of 2.1 meV/mV, corresponding to $\Delta E^{\ddagger} \simeq 0.103$ eV $\simeq 4kT$ at $U = 50$ mV, and $\tau_0 \simeq 4$ ms for the prefactor. Finally, Figure 6 illustrates that minute variations of the trap position z drastically change the occupation probabilities of the two states. This extreme fragility of the 50/50 occupation balance is theoretically explained by the above-mentioned exponential dependence of τ on $\Delta E^{\ddagger}$. In the future, we plan to exploit this sensitivity to further improve the resolution of our device.

In conclusion, our experiments provide convincing evidence that force controlled translocation dynamics of a (discretized) biopolymer through a NP is accompanied by a thermally induced, stochastic hopping between two adjacent NP states that can adequately be described by Kramers rate theory. Beyond the possibility to detect and reversibly control the position of a single translocating protein attached to a DNA strand, obviously the overall elasticity of the DNA-polymer significantly contributes to the retarded force response signals when threaded through a NP. With the current NP architecture a clear discrimination of two neighboring, close-packed proteins on a DNA-strand or, for example, of two adjacent nucleic acid bases is very difficult, and sets a serious limit for the possibility of force-controlled DNA mapping and sequencing applications. However, it will be interesting to pursue if, beyond the absolute force, the extremely sensitive and associated force fluctuation dynamics can be used to map or even sequence biopolymers like DNA during translocation. Further analysis concepts may either make use of a narrowed barrier between the NP states and/or a reduced distance between the two states by using thinner membranes (e.g., carbon nanosheets[22] or graphene[23]) as well as NPs with a much smaller pore diameter. In either case, these force controlled concepts will compete with Coulter counter based analysis concepts using protein NPs[5,24] or nanoelectric ratcheting devices[6] and make the topic of single molecule NP based spectroscopy and analysis very timely and promising.

AUTHOR INFORMATION

Corresponding Author

*E-mail: dario.anselmetti@physik.uni-bielefeld.de.

ACKNOWLEDGMENT

The authors would like to thank Cees Dekker, Armin Gölzhäuser, Wiebke Hachmann, Andreas Hütten, Maryam Khaksar, Paul Modrich, Christoph Pelargus, Karsten Rott,

Urs Staufer, and Katja Tönsing for valuable discussion and technical support. Financial support from the Deutsche Forschungsgemeinschaft within the Collaborative Research Center (SFB 613) is gratefully acknowledged.

REFERENCES

(1) Special Issue on "New developments in nanopore research - from fundamentals to applications", Albrecht, T.; Edel, J.B.; and Winterhalter, M.; Editors, *J. Phys.: Condens. Matter* **2010**, *45*, 450301–455106.

(2) (a) Han, J.; Fu, J.; Schoch, R. B. *Lab Chip* **2008**, *8*, 23–33. (b) Martin, C. R.; Siwy, Z. *Nat. Mater.* **2004**, *3*, 284–285. (c) Jirage, K. B.; Hulteen, J. C.; Martin, C. R. *Science* **1997**, *278*, 655–658.

(3) (a) Eftekhari, F.; Escobedo, C.; Ferreira, J.; Duan, X.; Girotto, E. M.; Brolo, A. G.; Gordon, R.; Sinton, D. *Anal. Chem.* **2009**, *81*, 4308–4311. (b) Harrell, C. C.; Choi, Y.; Horne, L. P.; Baker, L. A.; Siwy, Z. S.; Martin, C. R. *Langmuir* **2006**, *22*, 10837–10843. (c) Kim, Y. R.; Min, J.; Lee, I. H.; Kim, S.; Kim, A. G.; Kim, K.; Namkoong, K.; Ko, C. *Biosens. Bioelectron.* **2007**, *22*, 2926–2931. (d) Gu, L.-Q.; Shim, J. W. *Analyst* **2010**, *135*, 441–451. (e) Bayley, H.; Cremer, P. S. *Nature* **2001**, *413*, 226–230. (f) Sutherland, T. C.; Long, Y. T.; Stefureac, R. I.; Bediako-Amoa, I.; Kraatz, H. B.; Lee, J. S. *Nano Lett.* **2004**, *4*, 1273–1277.

(4) (a) Astier, Y.; Braha, O.; Bayley, H. *J. Am. Chem. Soc.* **2006**, *128*, 1705–1710. (b) Howorka, S.; Cheley, S.; Bayley, H. *Nat. Biotechnol.* **2001**, *19*, 636–639. (c) Akeson, M.; Branton, D.; Kasianowicz, J. J.; Brandin, E.; Deamer, D. W. *Biophys. J.* **1999**, *77*, 3227–3233. (d) Singer, A.; Wanunu, M.; Morrison, W.; Kuhn, H.; Frank-Kamenetskii, M.; Meller, A. *Nano Lett.* **2010**, *10*, 738–742. (e) Branton, D.; et al. *Nat. Biotechnol.* **2008**, *26*, 1146–1153.

(5) (a) Clarke, J.; Wu, H.-C.; Jayasinghe, L.; Patel, A.; Reid, S.; Bayley, H. *Nat. Nanotechnol.* **2009**, *4*, 265–270. (b) Derrington, I. M.; Butler, T. Z.; Collins, M. D.; Manrao, E.; Pavlenok, M.; Niederweis, M.; Gundlach, J. H. *Proc. Natl. Acad. Sci. U.S.A.* **2010**, *107*, 16060–16065.

(6) Luan, B.; Peng, H.; Polonsky, S.; Rossnagel, S.; Stolovitzky, G.; Martyna, G. *Phys. Rev. Lett.* **2010**, *104*, 238103.

(7) (a) Meller, A.; Nivon, L.; Brandin, E.; Golovchenko, J.; Branton, D. *Proc. Natl. Acad. Sci. U.S.A.* **2000**, *97*, 1079–1084. (b) Han, A. P.; Schurmann, G.; Mondin, G.; Bitterli, R. A.; Hegelbach, N. G.; de Rooij, N. F.; Staufer, U. *Appl. Phys. Lett.* **2006**, *88*, 093901. (c) Kowalczyk, S. W.; Hall, A. R.; Dekker, C. *Nano Lett.* **2010**, *10*, 324–328.

(8) (a) Schoch, R. B.; Han, J. Y.; Renaud, P. *Rev. Mod. Phys.* **2008**, *80*, 839–883. (b) Sparreboom, W.; van den Berg, A.; Eijkel, J. C. T. *Nat. Nanotechnol.* **2009**, *4*, 713–720.

(9) (a) Skinner, G. M.; van den Hout, M.; Broekmans, O.; Dekker, C.; Dekker, N. H. *Nano Lett.* **2009**, *9*, 2953–2960. (b) Smeets, R. M. M.; Kowalczyk, S. W.; Hall, A. R.; Dekker, N. H.; Dekker, C. *Nano Lett.* **2009**, *9*, 3089–3095.

(10) Hall, A. R.; van Dorp, S.; Lemay, S. G.; Dekker, C. *Nano Lett.* **2009**, *9*, 4441–4445.

(11) (a) Sischka, A.; Kleimann, C.; Hachmann, W.; Schäfer, M. M.; Seuffert, I.; Tönsing, K.; Anselmetti, D. *Rev. Sci. Instrum.* **2008**, *79*, 063702. (b) Sischka, A.; Spiering, A.; Khaksar, M.; Laxa, M.; König, J.; Dietz, K.-J.; Anselmetti, D. *J. Phys.: Condens. Matter* **2010**, *22*, 454121.

(12) (a) Bustamante, C.; Marko, J. F.; Siggia, E. D.; Smith, S. *Science* **1994**, *265*, 1599–1600. (b) Marko, J. F.; Siggia, E. D. *Macromolecules* **1995**, *28*, 8759–8770. (c) Berkovich, R.; Garcia-Manyes, S.; Urbakh, M.; Klafter, J.; Fernandez, J. M. *Biophys. J.* **2010**, *98*, 2692–2701.

(13) (a) Hagerman, P. J. *Annu. Rev. Biophys. Biophys. Chem.* **1988**, *17*, 265–286. (b) Ritort, F. *J. Phys.: Condens. Matter* **2006**, *18*, R531–R583.

(14) Cummings, E. B.; Griffiths, S. K.; Nilson, R. H.; Paul, P. H. *Anal. Chem.* **2000**, *72*, 2526–2532.

(15) (a) Hänggi, P.; Talkner, P.; Borkovec, M. *Rev. Mod. Phys.* **1990**, *62*, 251–341. (b) Reimann, P. *Phys. Rep.* **2002**, *361*, 57–265.

(16) (a) Evans, E.; Ritchie, K. *Biophys. J.* **1997**, *72*, 1541–1555. (b) Hummer, G.; Szabo, A. *Biophys. J.* **2003**, *85*, 5–15. (c) Dudko, O. K.; Filippov, A. E.; Klafter, J.; Urbakh, M. *Proc. Natl. Acad. Sci. U.S.A.* **2003**, *100*, 11378–11381.

(17) (a) Ghosal, S. *Phys. Rev. E: Stat. Nonlin. Soft Matter Phys.* **2007**, *76*, 061916. (b) Ghosal, S. *Phys. Rev. Lett.* **2007**, *98*, 238104. (c) van Dorp, S.; Keyser, U. F.; Dekker, N. H.; Dekker, C.; Lemay, S. G. *Nat. Phys.* **2009**, *5*, 347–351.

(18) Long, D.; Viovy, J. L.; Ajdari, A. *Phys. Rev. Lett.* **1996**, *76*, 3858–3861.

(19) (a) Keyser, U. F.; Koeleman, B. N.; Van Dorp, S.; Krapf, D.; Smeets, R. M. M.; Lemay, S. G.; Dekker, N. H.; Dekker, C. *Nat. Phys.* **2006**, *2*, 473–477. (b) Luan, B. Q.; Aksimentiev, A. *Phys. Rev. E* **2008**, *78*, 021912.

(20) (a) Woodhead, J. L.; Malcolm, A. D. B. *Nucleic Acids Res.* **1980**, *8*, 389–402. (b) Sidorova, N. Y.; Rau, D. C. *J. Mol. Biol.* **2001**, *310*, 801–816.

(21) Story, R. M.; Weber, I. T.; Steitz, T. A. *Nature* **1992**, *355*, 318–325.

(22) Turchanin, A.; Beyer, A.; Nottbohm, C. T.; Zhang, X.; Stosch, R.; Sologubenko, A.; Mayer, J.; Hinze, P.; Weimann, T.; Gölzhäuser, A. *Adv. Mater.* **2009**, *21*, 1233–1237.

(23) (a) Schneider, G. F.; Kowalczyk, S. W.; Calado, V. E.; Pandraud, G.; Zandbergen, H. W.; Vandersypen, L. M. K.; Dekker, C. *Nano Lett.* **2010**, *10*, 3163–3167. (b) Merchant, C. A.; Healy, K.; Wanunu, M.; Ray, V.; Peterman, N.; Bartel, J.; Fischbein, M. D.; Venta, K.; Luo, Z.; Johnson, A. T. C.; Drndic, M. *Nano Lett.* **2010**, *10*, 2915–2921.

(24) Deamer, D. *Annu. Rev. Biophys.* **2010**, *39*, 79–90.